

Simultaneous monitoring of the photometric and polarimetric activity of the young star PV Cep in the optical/near-infrared bands ¹

D.Lorenzetti¹, T.Giannini¹, V.M.Larionov^{2,3,4}, A.A.Arkharov³, S.Antoniucci¹, A.Di Paola¹, T.S.Konstantinova², E.N.Kopatskaya², G.Li Causi¹, and B.Nisini¹

ABSTRACT

We present the results of a simultaneous monitoring, lasting more than 2 years, of the optical and near-infrared photometric and polarimetric activity of the variable protostar PV Cep. During the monitoring period, an outburst has occurred in all the photometric bands, whose declining phase ($\Delta J \approx 3$ mag) lasted about 120 days. A time lag of ~ 30 days between optical and infrared light curves has been measured and interpreted in the framework of an accretion event. This latter is directly recognizable in the significant variations of the near-infrared colors, that appear bluer in the outburst phase, when the star dominates the emission, and redder in declining phase, when the disk emission prevails.

All the observational data have been combined to derive a coherent picture of the complex morphology of the whole PV Cep system, that, in addition to the star and the accretion disk, is composed also by a variable biconical nebula. In particular, the mutual interaction between all these components is the cause of the high value of the polarization ($\approx 20\%$) and of its fluctuations.

The observational data concur to indicate that PV Cep is not a genuine EXor star, but rather a more complex object; moreover the case of PV Cep leads to argue about the classification of other recently discovered young sources in outburst, that have been considered, maybe over-simplifying, as EXor.

¹INAF - Osservatorio Astronomico di Roma, via Frascati 33, 00040 Monte Porzio, Italy, lorenzetti, giannini, antoniucci, dipaola, licausi, nisini@oa-roma.inaf.it

²Astronomical Institute of St.Petersburg University, Russia, vlar2@yandex.ru, azt8@mail.ru, enik1346@rambler.ru

³Central Astronomical Observatory of Pulkovo, Pulkovskoe shosse 65, 196140 St.Petersburg, Russia, arkadi@arharov.ru

⁴Isaac Newton Institute of Chile, St.Petersburg branch

Subject headings: Stars: pre-main sequence – variable – emission lines – individual: PV Cep – ISM: jets and outflows – infrared: stars

1. Introduction

PV Cephei ($\alpha_{2000} = 20^h45^m53.96^s$, $\delta_{2000} +67^\circ57'38.9''$) is a pre-main sequence star in the northeastern edge of the L1158 and L1155 group of dark clouds, at a distance of about 500 pc (Cohen et al. 1981). It underwent significant short lived outbursts detected in the optical and near IR bands, and, therefore, it was classified as an EXor object (Herbig 1989). The commonly accepted spectral type of PV Cep is A5 (see e.g. Ábrahám et al. 2000 and references therein), but, during local minimum, it shows an absorption spectrum attributable to a later spectral type G8-K0 (Magakian & Movsesian 2001). Indeed, its nature has been never certainly stated, although it has been studied in several occasions and at different frequencies: sometimes it has been classified as an Herbig Ae star (e.g. Fuente et al. 2002), or as a FUor system. No doubt it is an embedded young object whose phenomenology is partly attributable to recurrent accretion from the circumstellar disk (Hartmann & Kenyon 1985). With this respect, the existence of an edge-on circumstellar disk was indirectly suggested by the presence of ice absorption in the 2-4 μm spectrum (Van Citters & Smith 1989). A more recent interferometric observation at 1.3 and 2.7 mm has been able to resolve a relatively large (500 AU) and massive ($0.8 M_\odot$) disk (Hamidouche 2010).

According to a widely accepted picture, these systems accrete material from their disks through rapid and intermittent events that generate thermal instabilities in the disk itself and, eventually, outbursts phenomena. Accreted matter migrates toward the central star where it is channelled along the magnetic field lines (e.g. Shu et al. 1994). The fall onto the stellar surface produces a shock that cools by emitting a hot continuum; moreover, as a consequence of the accretion event, strong winds (in some cases also collimated jets) emerge from the rotating star/disk system. Accretion disks survive few million years before dissipating, thus it is plausible that accretion events go on for a period shorter than that, with an outburst intensity that decreases with time.

The interaction with a close binary companion is also invoked as an alternative mechanism to produce accretion disk instabilities and consequent outbursts (Clarke, Lin & Pringle 1990; Bonnell & Bastien 1992), but recent IR surveys (even with adaptive optics) for search-

¹Based on observations collected at AZT-24 telescope (Campo Imperatore, Italy), AZT-8 (Crimea, Ukraine), and LX-200 (St.Petersburg, Russia)

ing a binary close to PV Cep (Connelley, Reipurth & Tokunaga 2008, 2009) have given a negative result.

PV Cep is associated with GM-29 (RNO 125), an optically visible (Cohen et al. 1977; Gyul’budagyan & Magakyan 1977) and infrared (Connelley, Reipurth & Tokunaga 2007) variable nebula (with an intermittent north-east streak) whose very rapid changes (both in brightness and in morphology) are more likely due to a variable illumination from the star rather than to an intrinsic phenomenon. Infrared analogs are the variable nebulae associated with both the protostar L483 (Connelly, Hodapp, & Fuller 2009) and the eruptive object V1647 Ori (Briceño et al. 2004; Fedele et al. 2007).

PV Cep drives the giant HH 315 flow (Gómez, Kenyon & Whitney 1997; Reipurth, Bally & Devine 1977) and a molecular outflow (Levreault 1984, 1988), both aligned with the symmetry axis of the nebula at a position angle of 330° . The blue-shifted ^{13}CO integrated emission shows a V-shaped morphology coincident with the reflection nebula, while the blue-shifted ^{12}CO traces fan-like morphology that fills the cavity delineated by the ^{13}CO structure (Arce & Goodman 2002). These latter authors suggest that the ^{13}CO traces the limb-brightened walls of a wide-angle wind blown cavity.

Large values of intrinsic polarization ($\approx 10\text{-}15\%$) and evidence of polarimetric variability were detected by Bastien & Ménard (1988) and Ménard & Bastien (1992). In the period 1981-1989, polarization maps were obtained by Gledhill et al. (1987) and Scarrott et al. (1991), who proposed a model for the PV Cep/GM29 system according which: *(i)* the main characteristic of the system is its rapid brightness and structural variability, sometimes on the time-scale of months; *(ii)* the intermittent north-east streak is a reflection effect caused by sporadic illumination of the outer parts of the cavity wall by radiation from the central star; *(iii)* the star is seen through at least two sets of polarizing grains with different alignments and the relative amount of extinction by each set has changed with time.

We have started our monitoring of PV Cep since some years, and part of the data have been already presented in Larionov et al. (2007) and Arkharov et al. (2008). The present paper deals with a more than 2 years, multi-wavelength monitoring (visual, near-IR photometry and I-band polarimetry), during which PV Cep underwent an outburst followed by a very rapid and significant declining; our aim is put the complex phenomenology of PV Cep into a coherent scheme.

Quite recently, the results of an optical (V,R,I) monitoring of PV Cep have been presented (Kun et al. 2011) complemented with some *Spitzer* mid-IR photometric data. Their optical light-curves present an overlap with ours although they cover a longer period: within the overlapping region their data are fully in agreement with those presented here; near-IR data are substantially our data retrieved from literature. Kun et al. (2011) suggest that the

photometric decline they have sampled resulted from an interplay between variable accretion and circumstellar extinction. A comparative analysis between their and our conclusions will be done in the following (Sects. 3.1.2, 3.3, 3.4 and 4).

The paper is structured as follows: in Sect.2 the observations are presented, while in Sect.3 the results are provided in the context of the previous knowledge of this source. Finally, our conclusions are summarized in Sect.4.

2. Observations

All the observations (see also Table 2 in Appendix) were obtained during the period April 2007 - Nov. 2009. Noticeably, the intra-day or day time-scale variations are not relevant for the discussion, so that observations in different bands have been associated to the same date (within a maximum distance of 1 day) even if not strictly simultaneous.

2.1. Optical photometry and polarimetry

Optical photometric and polarimetric observations were obtained with two nearly-identical photometers-polarimeters of the Astronomical Institute of St.Petersburg University, mounted on the 70cm AZT-8 telescope of the Crimean Observatory (Ukraine) and 40cm LX-200 telescope of St.Petersburg University, respectively. These photometers are based on ST-7XME SBIG CCDs and equipped with UBV (Johnson) and RI (Cousins) filters. In polarimetric mode two Savart plates are used as analyzers, giving q and u Stokes parameters. AZT-8 observations were obtained in R and I bands, while LX-200 ones in unfiltered mode, whose effective wavelength roughly corresponds to the R band. The pixel scale is 0.64 arcsec/pxl which corresponds to a 8.1×5.4 arcmin² field of view.

The optical light curves are given in the three upper panels of Figure 1 for the V, R, and I band, respectively, while the polarimetric results are listed in Table 2 of the Appendix.

2.2. Near-IR photometry

Near-IR data were obtained at the 1.1m AZT-24 telescope located at Campo Imperatore (L'Aquila - Italy) equipped with the imager/spectrometer SWIRCAM (D'Alessio et al. 2000), which is based on a 256×256 HgCdTe PICNIC array. Photometry is performed with broad band filters J ($1.25 \mu\text{m}$), H ($1.65 \mu\text{m}$), and K ($2.20 \mu\text{m}$). The total field of view is 4.4×4.4 arcmin², which corresponds to a plate scale of 1.04 arcsec/pixel. All the

observations were obtained by dithering the telescope around the pointed position. The raw imaging data were reduced by using standard procedures for bad pixel removal, flat fielding, and sky subtraction. The derived light curve is depicted in the three lower panels of Figure 1 for the J, H, and K band, respectively.

3. Results and discussion

3.1. Amplitude and colors variations

3.1.1. Near-infrared colors

PV Cep light-curves presented in Figure 1 show how the source has undergone a significant variability during the monitoring period of more than 2 yr. In particular a rapid (~ 120 days) and significant ($\Delta J \gtrsim 3$ mag) declining is evident between MJD 54558 and 54673 (even if with a short rising lasting about 10 days).

Aiming at investigating the possible origin of the photometric variations, we plot in Figure 2 the near-IR [J-H] vs [H-K] color diagram of PV Cep. All the data cluster in the red portion of the plot, but important differences exist. To indicate the star bright and faint states we have marked with blue (red) dots the points with J-magnitudes lesser (greater) than 11.0 (12.5), while black dots indicate J-magnitudes between these two. From the diagram it is quite evident the PV Cep becomes bluer (redder) while brightening (fading). This variability cannot be explained just with an extinction variation: in the same Figure we have depicted two different extinction laws (Rieke & Lebfosky 1989 and Cardelli et al. 1989): the points are not aligned with any extinction curve, but exhibit a clear shift to the right, that increases with decreasing the PV Cep brightness.

We have searched also for different mechanisms as a possible origin of the near-IR colors deviation. The scattering contribution has been evaluated following the relationships (2) and (3) given in Massi et al. (1999), valid for optically thin ($\tau_0 < 1$) dust producing an isotropic Rayleigh scattering. The scattering contribution for values of τ_0 between 0.1 and 1 produces color changes of just one tenth of magnitude. Finally, we have considered the effect of a hot spot on the stellar surface. As example we have assumed a hot spot temperature of $T=12000\text{K}$ and a surface equal to 40% of the stellar one, finding just negligible changes of near-IR colors (few hundredths of magnitudes).

Summarizing, from this part of the analysis we can deduce that: *i*) the color variations do not follow the extinction vector and are thus not due varying extinction, while the colors are reddened by a roughly constant extinction A_V of about 5-7 mag; *ii*) the range of the

color variations is similar in both colors (~ 0.8 mag); *iii*) the observed variations reflect an intrinsic phenomenon, likely due to the circumstance that, when outbursting, the central star becomes more visible, while when declining, the disk dominates; *iv*) the observed variations cannot be accounted for just by extinction fluctuations; other phenomena, such as scattering variations and/or hot spots on the stellar surface give negligible contributions.

3.1.2. Optical colors

It is worthwhile to repeat the above analysis by using the optical colors V, R, and I, where extinction and scattering are both expected to play a major role (Figure 3). In analogy with the near-infrared diagram, we indicate with blue (red) dots the points corresponding to high (low) brightness, identified with a V-band magnitude lesser (greater) than 17.7 (18.7). All data points roughly cluster in a locus corresponding to a main sequence A5 (K0) star extinguished by 6-7 (5-6) mag: this is what suggested also by near-IR colors and exactly what is expected for PV Cep (see Sect.1).

The well defined color segregation shown by PV Cep in the near-IR, appears here barely recognizable. We ascribe this difference to a combination of two facts: *(i)* the reduced effect (at visual wavelengths) of the intrinsic IR excess; *(ii)* the presence of additional contributions that, while negligible in IR, become important in the optical. For example (Figure 3, bottom right corner), the effect of a variable scattering (with τ_0 values from 0.1 to 1), gives color fluctuations compatible with a variable scattering nebula. Similarly, the presence of a hot spot on the star surface, with the same physical characteristics as those considered in the near-IR, gives substantial variations of about 0.5 mag in both colors. Remarkably, the optical colors are completely inconsistent with A_V variations in the range 7-15 mag, thus confirming what suggested by the near-IR plot. This comparison rules out the occurrence of large A_V changes and further demonstrates how the near-IR color variations cannot be due to extinction variations, but are originated by an intrinsic excess fluctuations.

Summarizing, from the VRI two colors plot we can deduce that: *i*) irrespectively of the adopted extinction law, A_V could be allowed to vary only in the range 6-8 mag; *ii*) other phenomena (than extinction) may have a significant role; *iii*) the range of the [V-R] color variations (> 1 mag) is significantly larger than that of [R-I] variations (~ 0.5 mag).

A different conclusion, in favour of an A_V component of about 3 mag, has been reached by Kun et al. (2011) through the analysis of their light-curves. This discrepancy may be due to the lack of simultaneity between their optical and near-IR photometry. Indeed, it is just the comparative analysis between optical and near-IR color plot that allowed us to rule out

any A_V variation during our monitoring period. In our opinion, this circumstance represents a clear example of how a simultaneous and multi-frequency monitoring of several brightening and fading events will lead to a more comprehensive conclusion, ie. not too related to the nature of single events.

3.2. Time delay in the light curve

By examining the light curves in different bands (Figure 1) some delay seems to exist between optical and near-IR observations, namely any event (characterized by an increasing or decreasing flux) appears to take place before at shorter wavelengths (see the black vertical dotted line in Figure 1). However, the possible existence of a temporal lag has to be supported in a more quantitative way. The common way to estimate delays between two light curves at different wavelengths is to use the Discrete Correlation Function (DCF - Edelson & Krolik, 1988). This method is suitable for measuring correlation functions when the sampling time is difficult to control (e.g. objects observed in different bands at different phases). The robustness of the DCF has been demonstrated by Hufnagel & Bregman (1992), who pointed out how the shape of the DCF reflects the underlying nature of the process to which the data refer. The parameters of the DCF are the width, that indicates the duration of the correlated phenomena between the two data sets, and the peak height, that is a measure of the correlation strength. To estimate delays between optical (R band) and near-IR (J band) we used the data in the time interval from MJD 545500 to MJD 54750, most densely covered in both bands. Our computation indicates (at a DCF level of about 40%, see Figure 4) that variations in the J band occur around 30 days after those in the R band.

The existence of a lag between optical and near-IR light-curves can be proved also in other YSO's. For example, Audard et al. (2010) have qualitatively recognized some lag between the near-infrared and optical light curves of the EXor variable V1118 Ori: we have applied the DCF method to their data (their Table 2) obtaining the same lag of about 30 days, with a larger DCF peak $\lesssim 0.7$. The similarity of the lag duration speaks in favor of a common mechanism responsible for these phenomena. Likely, we are simply looking at the response of the emitting matter at each frequency (regulated by its thermal capacitance) when it is undergoing an heating by outburst or a cooling. If this is the case, the practical constance of this lag should be a characteristics typical of any outbursting or declining event of any disk-accreting protostar: to this end, a careful investigation of the available optical/near-IR light curves should be desirable. We remark that the lag occurrence is not in agreement with an extrinsic variation eg. due to a circumstellar or interstellar dust screen (such as proposed by Kun et al. 2011), which would generate strictly simultaneous fluctuations at different

frequencies. Conversely, the lag supports the occurrence of an intrinsic phenomenon on the stellar surface (such as an accretion event or an irregular hot spot) that requires, because of its nature, a longer time to reach the maximum emission at longer wavelengths.

3.3. Polarization

The PV Cep polarization (P) data collected before our monitoring are listed in Table 1. Although these data stem from a random sampling obtained at different epochs (from 1980 to 1989) and in different bands, they indicate the large spread of observed values on short time-scales, and a long term increasing (on years time-scale) of the P maximum value. These qualitative indications have motivated us to systematically monitoring the polarization changes in PV Cep. To these new data (Table 2) refer the plots of Figure 5. Here the observed values of the polarization, its position angle (PA) along with the position angle of the main axis of the nebula (see below) are given as a function of time. The R (I) band polarization and PA values are marked as red (black) dots, while green dots represent polarization and PA values obtained in unfiltered mode. In the same plot the R-band light curve is also reproduced to make easy the comparison with the PV Cep brightness state.

We first note that the mean value of the polarization corresponding to our monitoring program is 19.5 %. This high P value is typical of a system viewed edge-on, like PV Cep: most of the light from the star is attenuated and the fraction of the scattered, polarized light, is high. Single or multiple scattering in optically equatorial thick disks and/or in the lobes of the associated bipolar nebulae are the widely accepted models to produce patterns of aligned polarization vector in YSO's (Bastien & Ménard 1988, 1990). The polarization maps of PV Cep (Gledhill et al. 1987; Scarrott et al. 1991) also agree with the proposed interpretation and their conclusions have been anticipated in Sect.1. However, whichever kind of scattering in disks cannot produce polarization values much larger than 12%, therefore single scattering in inhomogeneous dust distributions (such as bipolar nebulae) is additionally required (Daniel 1982).

Now we aim at understanding whether or not the observed polarization variations are statistically significant and, eventually, at inferring on the plausible causes of such variability.

To evaluate if polarization can be declared variable (within the errors), we adopt the prescription given by Ménard & Bastien (1992), namely a 95% confidence level established with a χ^2 test of the Stokes parameters within a given pass-band. The resulting $P(\chi^2)$ in our case is > 99.9 %, hence PV Cep can be considered a polarimetric variable. This result is well in agreement with the conclusion of the previous section 3.1 in favor of a varying scattering

(i.e. polarizing) nebula.

No clear correlation can be found between the polarization and either the brightness in all the observed photometric bands or the position angle of the polarization itself (PA, see Figure 5). These circumstances allow us to rule out some models that predict the origin of the polarimetric variations as uniquely due to accretion processes. Wood et al. (1996) investigated the photo-polarimetric variability of a magnetic accretion disk model for pre-main-sequence T Tauri stars. They find that matter from the disk accretes along the magnetic field lines onto the stellar surface producing hot and polarized spots; stellar rotation causes the photometric and polarimetric variations. However, at variance with our observational data, such model predicts a correlation between brightness and polarization variations, these latter occurring on time-scales comparable to the stellar rotation period.

We also searched for some periodicity in the polarization variability, with indications of a positive result. To this aim we used the complete set of polarization observations, that spans for more than 2 years (Figure 6). The fit to the data points with a sinusoidal behaviour gives formally a period of 847 days and a peak amplitude of 2.1% with a reduced $\chi^2 = 2.7$. Hence, just one period of a pure sinusoid marginally (within 3σ) accounts for the polarization variability, whose periodicity is somehow presumable. A significant increase of the monitoring time is needed to confirm such preliminary indication, also considering that non-periodic variations of different origin are expected to occur. If this tentative interpretation were confirmed, it would suggest a period typical of a disk orbital motion or of a circumstellar envelope externally illuminated and arranged in an asymmetric geometry. Also a circumbinary envelope should be able to produce periodic polarization variations, but at a very reduced amplitude, less than 1% (Manset & Bastien 2001).

The variations of PA, although not correlated with those of the polarization amplitude, do not seem negligible, and show some regularity. We can speculate, they also could be related to the changes in geometry of the circumstellar material more than to density inhomogeneities or clumps in the thick disk. This latter could indeed produce apparently random variations of both the polarization and its position angle (Ménard & Bastien 1992).

By following Scarrott et al. (1991), we conclude that the strong values of both the mean value of the polarization and its variations could be due to the presence of at least two populations of polarizing grains, having different alignments and giving relatively different contributions. A fixed and relevant amount of polarization could be due to the thickness of the disk, and a variable (perhaps periodic) component could sit on top of it, generated by an asymmetrically organized circumstellar material.

3.4. The nebula

A photometric analysis of the (cometary) nebula associated to PV Cep is not a task afforded in the present paper. Here the aim is to put into light some phenomenology associated to the nebula that could contribute to form a more coherent picture of the overall PV Cep system. Our optical observations confirm that the northern part of the nebula (ie. the one associated to the blue CO lobe) is by far the brightest, while the southern one remains visible only in few periods. Moreover, the nebula brightness tends to rather closely correlate with the brightness of the object itself, confirming its illuminated nature. The time fluctuations in position of the nebula’s main axis θ_{neb} (Figure 5, bottom panel) are noticeable in the present context. This angle is computed (from N to E) as the position angle of the brightest portion of the fan, with a typical error of about 1-2°. In most cases, the brightest portion of the fan coincides with the nebula axis, although sometimes it is difficult to distinguish between the axis and the brightest blob. The computed values of θ_{neb} are given in the last column of Table 2. For a typical system composed by a bi-conical nebula emerging from an edge-on disk, the nebula axis is expected to be orthogonal to the disk itself; indeed, being the PV Cep disk on average oriented at 60° (see PA in Figure 5), the nebula’s axis presents a perpendicular average value of -30°, but showing huge and quite regular fluctuations of $\pm 30^\circ$.

Firstly, we can exclude that this sort of nebula’s axis precession (or brightest blob movement) is due to a changing illumination directly from the star (or from the disk), otherwise both would present similar fluctuations with a fixed delay determined by the light travelling time from the star to the blob (≈ 30 days). Suitable tests (DCF analysis) done to search for possible correlations provided negative results.

Instead, the nebula axis movement speaks in favor of some motion of crucial parts of the overall structure. We can hardly believe that the nebula or the disk are physically precessing in a so short time-scales, rather we are seeing a permanent movement of the hole (namely the innermost region of the disk itself) in the CS disk through which the light penetrates to illuminate the fan. Different portions of the walls delimiting the hole can plausibly reflect not uniformly the starlight, then originating systematic differences in the nebula illumination (see also Cohen et al. 1981). Such a mechanism is compatible with the time-scale of the observed θ_{neb} fluctuation that are of the order of 1-2 yrs; however our data do not cover a temporal range long enough to infer on a possible periodicity. Conversely, if the central star were the direct illuminator, the time-scale of θ_{neb} fluctuation should be reconcilable with much shorter time-scales (days) typical of the stellar dynamics (eg. rotation). According to the proposed scenario, θ_{neb} (ie. the orientation of the brightest part of the nebula) and PA (related to the grain orientation) are expected to be rather uncorrelated (as confirmed

by Figure 5. The proposed view agrees with the interpretation given by Kun et al. (2011), according to which the variable shape of the nebula is not only due to the fading of the star, but also due to the changing geometry of the dust distribution close to the star.

3.5. Comparison with the EXor objects

At this stage, after having derived some properties by our optical and near-IR observations, we can come back to the issue of the PV Cep classification (as Herbig Ae star or EXor system). It presents many differences with respect to the classical EXor like XZ Tau, UZ Tau, VY Tau, DR Tau, V1118 Ori, NY Ori, V1143 Ori, EX Lup (Herbig 1989, Lorenzetti et al. 2009). In the light of the presented data, the most relevant are: *i*) the bursts modality evidenced in the light curve, that does not present a rapid (weeks) increasing and slower (months /years) declining; *ii*) the existence of a circumstellar nebulosity (with a significant variability both in morphology and brightness), which is not a so common feature for EXor’s; *iii*) the high value of the foreground extinction; *iv*) the near-IR colors (see Figure 2) that show larger fluctuations than those exhibited by other Exor’s. Other differences stem from considerations presented in the literature: *i*) the relatively early spectral type usually attributed to PV Cep and its bolometric luminosity (about $100 L_{\odot}$ instead of a few or fractional solar luminosity; *ii*) the association with mass loss manifestation (in terms of CO outflow and HH jets) usually not detected in classical EXor’s (Lorenzetti et al. 2006, 2007); *iii*) the presence of a rather massive circumstellar material of $\approx 1 M_{\odot}$ (Osterloh & Beckwith 1995; Fuente et al. 1998); *iv*) the presence of a significant far-IR counterpart that dominates its luminosity (Ábrahám et al. 2000); *v*) the association with a radio continuum likely arising in the shocked-ionized gas (Anglada et al. 1992); *vi*) the presence of an H₂O maser source, although at a relatively large distance ($\approx 3 \cdot 10^{16}$ cm) from the visible star (Rodríguez et al. 1987; Sunada et al. 2007).

Conversely, the similarity with other EXor stems from *i*) being an emission line object; *ii*) interpreting the recurrent bursts as mainly due to disk accretion events.

Considering all the presented evidences it seems that PV Cep is indeed an object more massive and more complex than other EXor. It represents an example suggesting that the EXor classification is not longer adequately accounted for, especially in the context of the recent detections of outbursting embedded objects, that have been often referred, maybe over-simplifying, as EXor.

Most of these objects (such as V1647 Ori, OO Ser, EC 53, ISO ChaI 92, GM Cep)

are indeed more embedded (i.e. younger) than classical EXor. In principle, there is no conceptual reason which prevents the EXor phenomena to occur in a more embedded phase. This implies, however, that the well defined outburst modalities typical of visible, quite isolated, low mass objects, become unavoidably less recognizable. Consequently, the EXor class could include objects of different nature. If EXor were uniquely recognized to be YSO's undergoing random accretion phenomena (of some relevance in brightness variations), then almost all the YSO's (Class I objects, Herbig Ae/Be stars, active T Tauri stars) should be incorporated in that class, since they all present a random and significant variability.

4. Concluding remarks: a consistent picture

We have presented the results of a simultaneous monitoring, lasting more than 2 years, of the photometric and polarimetric activity of the young stellar object PV Cep, in the optical/near-IR bands. This work aimed at investigating its physical properties, the causes of its variability and the nature of this object. By analyzing the results, here we try to delineate a consistent picture of the PV Cep system.

PV Cep is a young Ae star with a quite massive circumstellar thick disk associated to a bi-conical and variable (both in brightness and in main axis direction) nebula. While the disk rotates (in a typical time-scale of 1-2 years) it could present a not homogeneous internal edge to the star light which, consequently, illuminates with a different intensity different portions of the nebula. Reasonable consequences of the mechanism described above are the recurrent brightness variations of the nebula along with those of its main axis, whose differences are also related to the disk rotation. The strong mean value on the polarization is due to the thick disk, while the variable (maybe periodic) component is related to the different illumination of the nebula itself.

In addition to these phenomena, recurrent disk accretion events have a role in producing intermittent outbursts in the light curve. By examining the light-curves given in Figure 1, we note PV Cep shows a significant variability (in a period of 2-3 years) during which an outburst has occurred, whose declining phase ($\Delta J \approx 3$ mag) lasted about 120 days. Such a time interval appears indeed short when compared with the classical declining times toward the quiescence exhibited by the EXor objects (typically months/years). Nevertheless, the occurrence of intermittent accretion events from the circumstellar disk onto the central star, that are widely accepted as the origin of EXor outbursts, cannot be ruled out just on the basis of the light-curve shape.

The near-infrared color variations of PVCep are similar to those of EXor, that tend

to be bluer when outbursting and redder when fading. This behaviour is likely due to the circumstance that when outbursting the central star becomes more visible, while when declining the disk dominates. As a result the near-IR colors related to accretion outbursts and those related to extinction variations have the same appearance.

At variance with other EXor objects (Lorenzetti et al 2009), the global behaviour from V to K bands indicates that PV Cep variations occur behind a not negligible foreground extinction ($A_V \sim 5-7$ mag). The accretion disk responsible for the near-infrared color variations does not influence the variations of the optical colors. On the contrary, the irregular fluctuations of these latter appear mainly influenced by scattering contributions due to the variable nebula. Possible contributions from small extinction variations and from the presence of hot spots could affect just the optical regime by provoking some *noise* in the corresponding colors.

The occurrence of accretion events is also supported by an observational fact that cannot be accounted for in a scheme of pure extinction variations. This fact is the time lag in the light-curves discussed in Sect.3.2. An extinction variation in fact, cannot determine any time delay between the optical and the near-IR outburst since it acts as a mere screen able to produce only simultaneous changes at any wavelength.

About the PV Cep classification, we conclude that it presents many differences with respect to the known EXor and we believe it is an object more massive and more complex than other EXor. The case of PV Cep could lead to argue about the classification of some recently discovered young sources in outburst, that are referred, maybe over-simplifying, as EXor.

Noticeably, some of our conclusions, although reached in a completely different way, substantially agree with those traced by Kun et al. (2011). These concern the important role of accretion, the origin of the nebula variations, the presence of a not homogeneous components in the inner disk, the fact PV Cep differs from EXor type stars; on the contrary, their hypothesis of a variable extinction remains controversial.

5. Acknowledgements

The authors would like to thank Fabrizio Massi for helpful discussions on scattering properties and Riccardo Leoni for the support given during part of the observations at Campo Imperatore.

REFERENCES

- Ábrahám, P., Leinert, Ch., Burkert, A. et al. 2000 A&A 354, 965
- Anglada, G., Rodríguez, L.F., Cantó, J. et al. 1992 ApJ 395, 494
- Arce, H.G. & Goodman, A.A. 2002 ApJ 575, 911
- Arkharov, A.A., Larionov, V.M, Leoni, R. et al. 2008 Astronomer’s Telegram #1607
- Audard, M., Stringfellow, G.S., Güdel, M. et al. 2010 A&A 511, 63
- Bastien, P. & Ménard, F. 1988 ApJ 326, 334
- Bastien, P. & Ménard, F. 1990 ApJ 364, 232
- Bonnell, L. & Bastien, P. 1992 ApJ 401, L31
- Briceño, C., et al. 2004 ApJ 606, L123
- Cardelli, J.A., Clayton, G.C. & Mathis, J.S. 1989 ApJ 345, 245
- Clarke, C., Lin, D. & Pringle, J. 1990 MNRAS 242, 439
- Cohen, M., Kuhl, L. & Harlan, E. 1977 ApJ 215L, 127
- Cohen, M., Kuhl, L. & Harlan, E. & Spinard, H. 1981 ApJ 245, 920
- Connelley, M.S., Hodapp, K.W. & Fuller, G.A. 2009 AJ 137, 3494
- Connelley, M.S., Reipurth, B. & Tokunaga, A.T. 2007 AJ 133, 1528
- Connelley, M.S., Reipurth, B. & Tokunaga, A.T. 2008 AJ 135, 2496
- Connelley, M.S., Reipurth, B. & Tokunaga, A.T. 2009 AJ 138, 1193
- D’Alessio, F., et al. 2000 Proc. of the SPIE Symp. on *Astronomical Telescopes and Instrumentation*, eds. M. Iye & A.F.M. Moorwood, 4008, 748
- Daniel, J.-Y. 1982 A&A 111, 58
- Edelson, R.A., & Krolik, J.H., 1988, ApJ, 333, 646
- Fedele, D., van den Ancker, M.E., Petr-Gotzen, M.G. et al. 2007 A&A 387, 977
- Fernie, J.D. 1983 PASP 95, 782

- Fuente, A., Martin-Pintado, J., Bachiller, R., Neri, R., Palla, F. 1998 A&A 334, 253
- Fuente, A., Martin-Pintado, J., Bachiller, R. et al. 2002 A&A 472, 199
- Gledhill, T.M., Warren-Smith, R.F. & Scarrott, S.M. 1987 MNRAS 229, 643
- Gyul’budagyan, A., & Magakyan, T. 1977 Sov. Astron. Lett. 3, 58
- Gómez, M., & Kenyon, S., Whitney, B.A. 1997 AJ 114, 265
- Hamidouche, M. 2010 ApJ 722, 204
- Hartmann, L. & Kenyon, S. 1985 ApJ 299, 462
- Herbig, G.H. 1989 Proc. of the ESO Workshop on *Low Mass Star Formation and Pre-Main Sequence Objects*, ed. B. Reipurth, p.233
- Hufnagel, B.R., & Bregman, J.N., 1992, ApJ, 386, 473
- Kun, M., Szegedi-Elek, E., Moór, A. et al. 2011 astro-ph, arXiv:1101.2329
- Larionov, V.M., Kopatskaya, E.N., Larionova, L.V. et al. 2007 Astronomer’s Telegram #1256
- Levreault, R.M. 1984 ApJ 277, 634
- Levreault, R.M. 1988 ApJ 330, 897
- Lorenzetti, D., Giannini, T., Calzoletti, L. et al. 2006 A&A 453, 579
- Lorenzetti, D., Giannini, T., Larionov, V.M. et al. 2007 ApJ 665, 1193
- Lorenzetti, D., Larionov, V.M., Giannini, T. et al. 2009 ApJ 693, 1056
- Magakian, T, & Movsesian, T.A. 2001 Astrophysics 44, 419
- Manset, N., & Bastien, P. 2001 AJ 122, 2692
- Massi, F., Giannini, T., Lorenzetti, D. et al. 1999 A&A Supp. 136, 471
- Ménard, F. & Bastien, P. 1992 AJ 103, 564
- Meyer, M.R., Calvet, N. & Hillenbrand, L.A. 1997 AJ 114, 288
- Osterloh, M. & Beckwith, S.V.W. 1995 ApJ 439, 288
- Reipurth, B., Bally, J. & Devine, D. 1997 AJ 114, 2708

- Rieke, G.H. & Lebofsky, M.J. 1985 ApJ 288, 618
- Rodríguez, L.F., Haschick, A.D., Torrelles, J.M, & Myers, P.C. 1987 A&A 186, 319
- Scarrott, S.M., Rolph, C.D. & Tadhunter, C.N. 1991 MNRAS 249, 131
- Shu, F.H., Najita, J.R., Ostriker, E. et al. 1994 ApJ 429, 781
- Sunada, K., Nakazato, T., Ikeda, N. et al. 2007 PASJ 59, 1185
- Van Citters Jr., G.W. & Smith, S. 2010 ApJ 719, 1896
- Wood, K., Kenyon, S.J., Withney, B.A. & Bjorkman, J.E. 1996 ApJ 458, L79

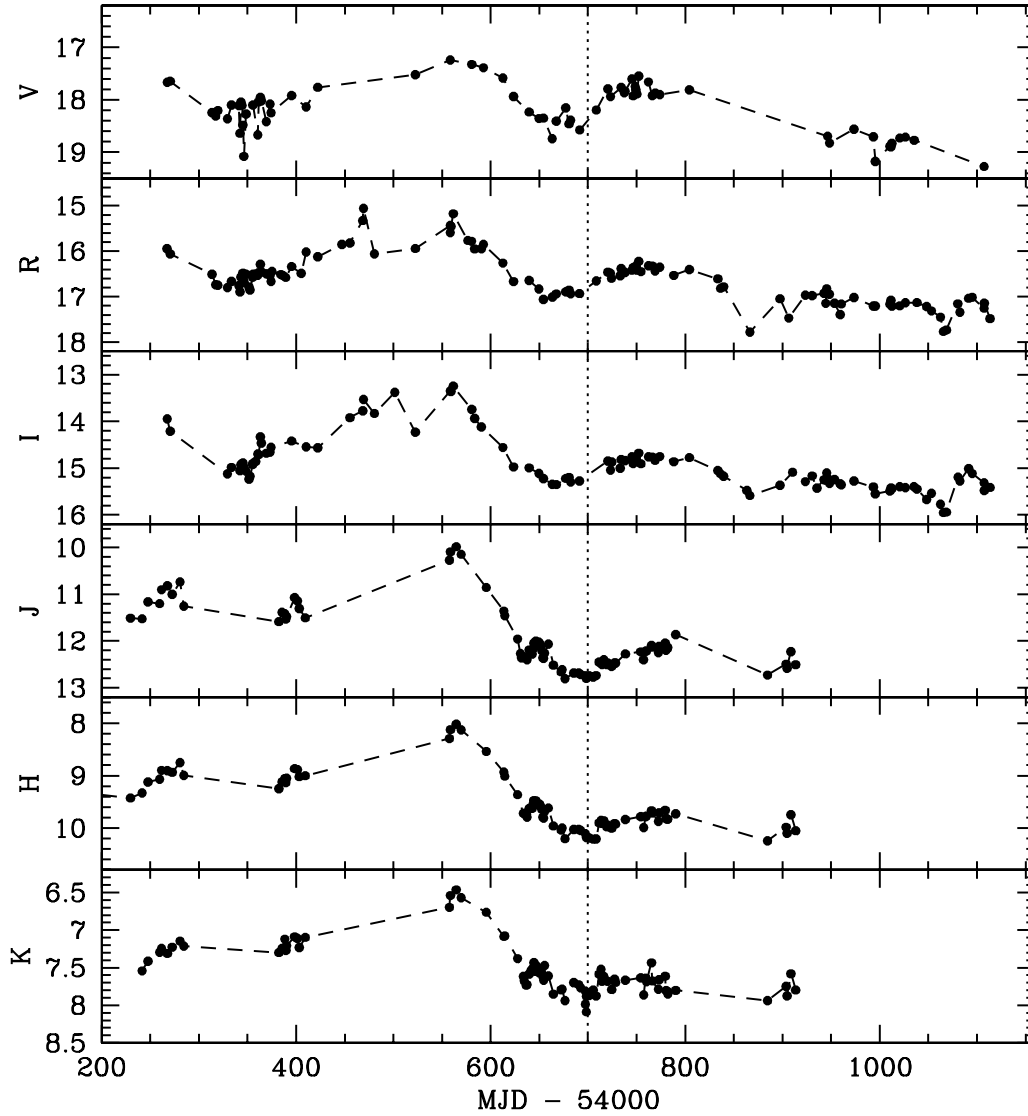


Fig. 1.— PV Cep optical and near-IR light curves vs. MJD (Modified Julian Date). The errors of data points are comparable to or lesser than 0.02 mag. The black vertical dotted line is plotted to have a temporal reference for a by-eye estimate of possible lags at different wavelengths.

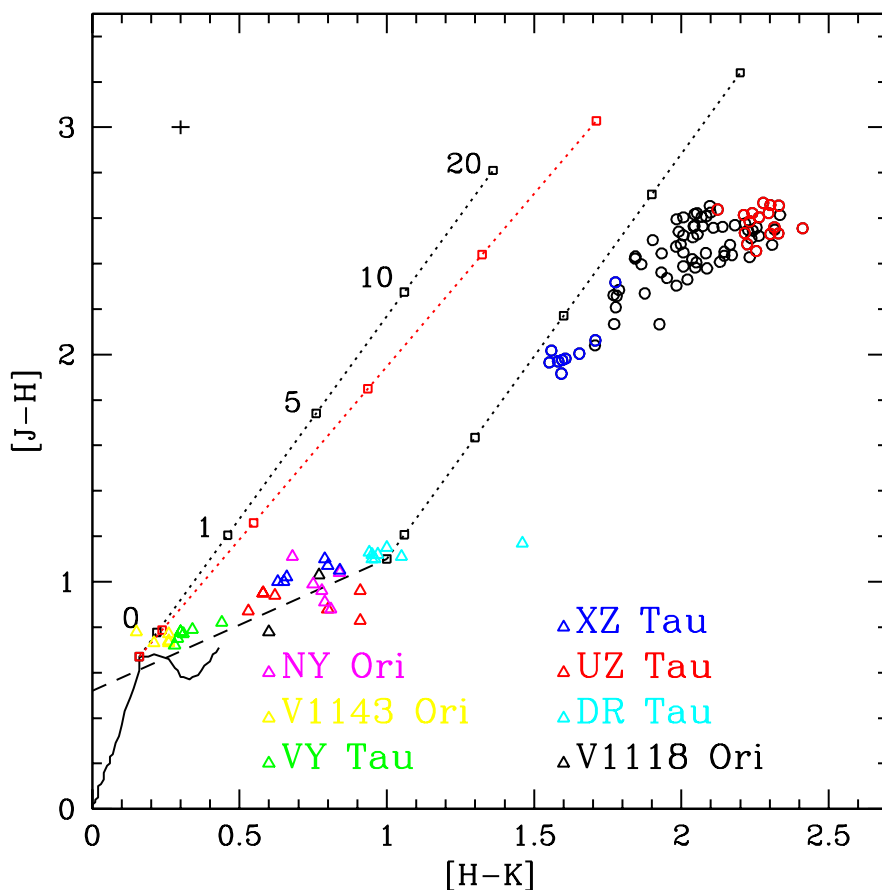


Fig. 2.— Near-IR two colors diagram of PV Cep in different epochs. The solid line marks the unreddened main sequence, whereas the dashed one is the locus of the T Tauri stars (Meyer et al. 1997). Black (red) dotted lines represent the reddening law by Rieke & Lebofsky (1985) and Cardelli et al. (1989), respectively, where different values of A_V are indicated by open squares. Blue (red) dots indicate those cases in which the source was found in its highest (lowest) state, arbitrarily identified with a J-band magnitude lesser (greater) than 11.0 (12.5). The near-IR colors of EXOr stars (Lorenzetti et al. 2009), that are targets of our on-going monitoring program, are also depicted with triangles and evidently overlap with the locus typical of T Tauri stars. A cross in the upper left corner indicates the typical error.

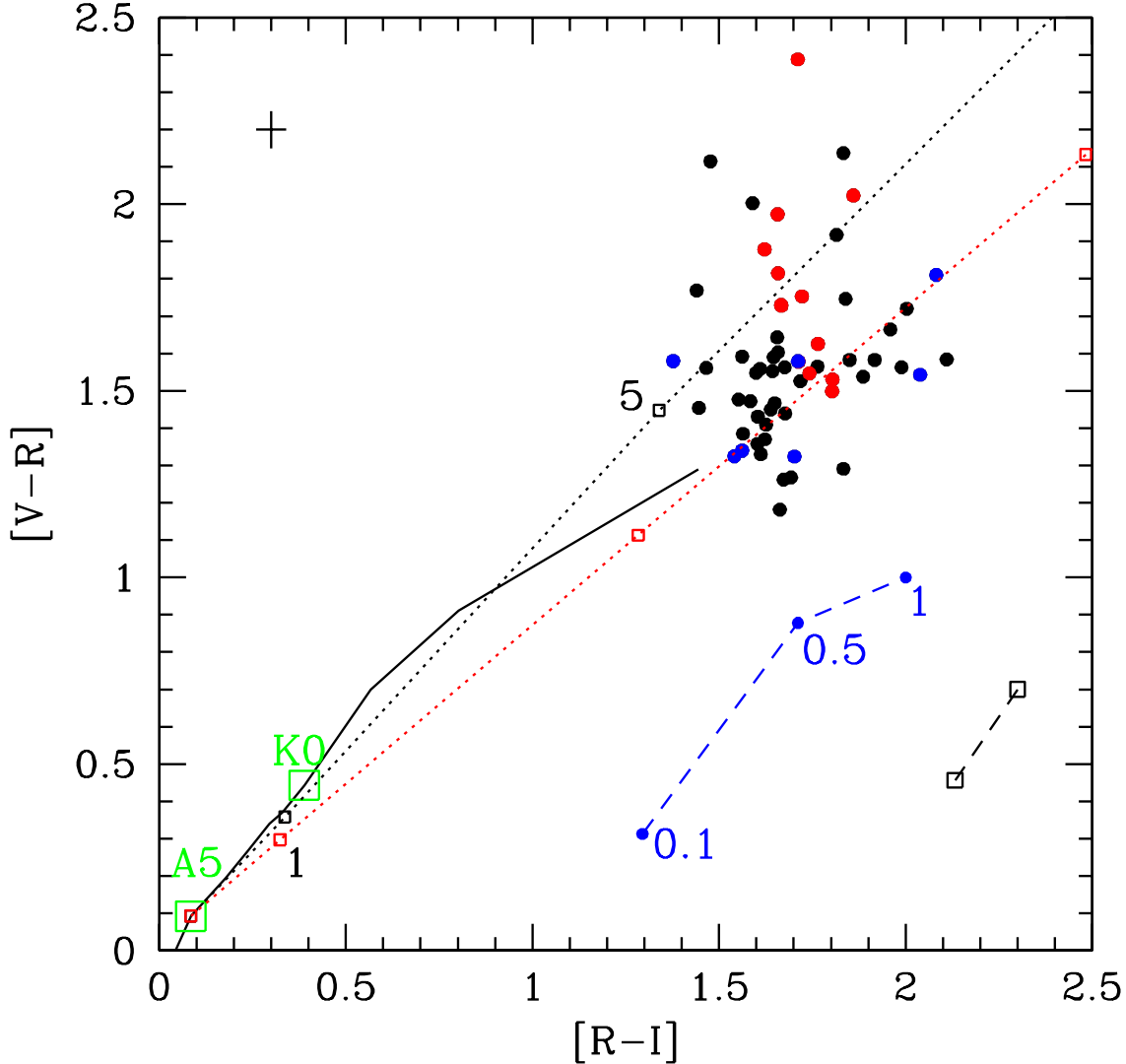


Fig. 3.— Visual two colors diagram of PV Cep in different epochs. The solid line marks the unreddened main sequence star of a given spectral type as defined by Kenyon & Hartmann (1995) and corrected from Johnson to Cousins system (Fernie 1983); the relevant (see text) spectral types A5 and K0 are indicated as green open squares. The black (red) dotted lines represent the reddening laws by Rieke & Lebofsky (1985) and Cardelli et al. (1989), respectively, where different values of A_V are indicated by open squares (0, 1, 5 mag). The blue curve arbitrarily applied on the bottom right represents the color variations shown by a given star for different values of the optical depth (τ_0) of the scattering nebula (from 1 to 0.1). By decreasing τ_0 (from 1 to 0.1) the scattering contribution increases and the star appears bluer. Blue (red) dots indicate those cases in which the source was found in its highest (lowest) state, arbitrarily identified with a V-band magnitude lesser (greater) than 17.7 (18.7). In the bottom right corner the blueing effect of adding a hot spot (having $T = 12000$ K and a surface equal to 40% of the stellar one) to an arbitrary point, is quantitatively indicated with squares. Finally, a cross in the upper left corner indicates the typical error.

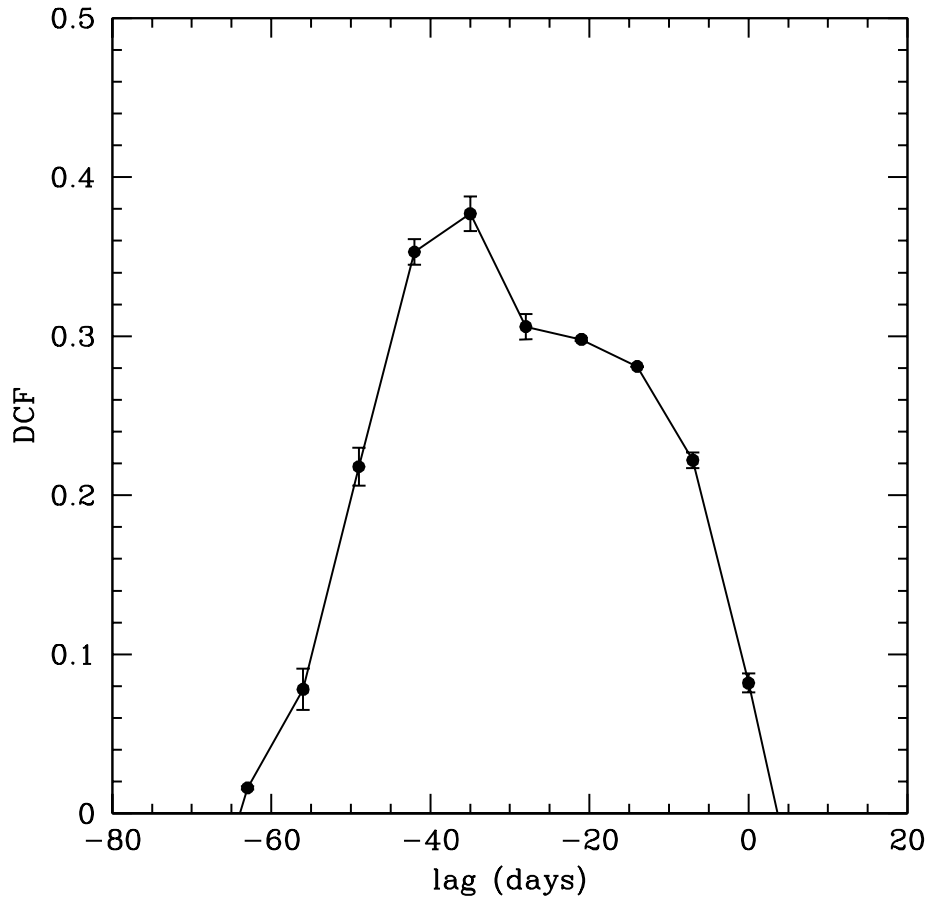


Fig. 4.— Discrete Correlation Function (DCF) for PV Cep optical (R band) and near-IR (J band).

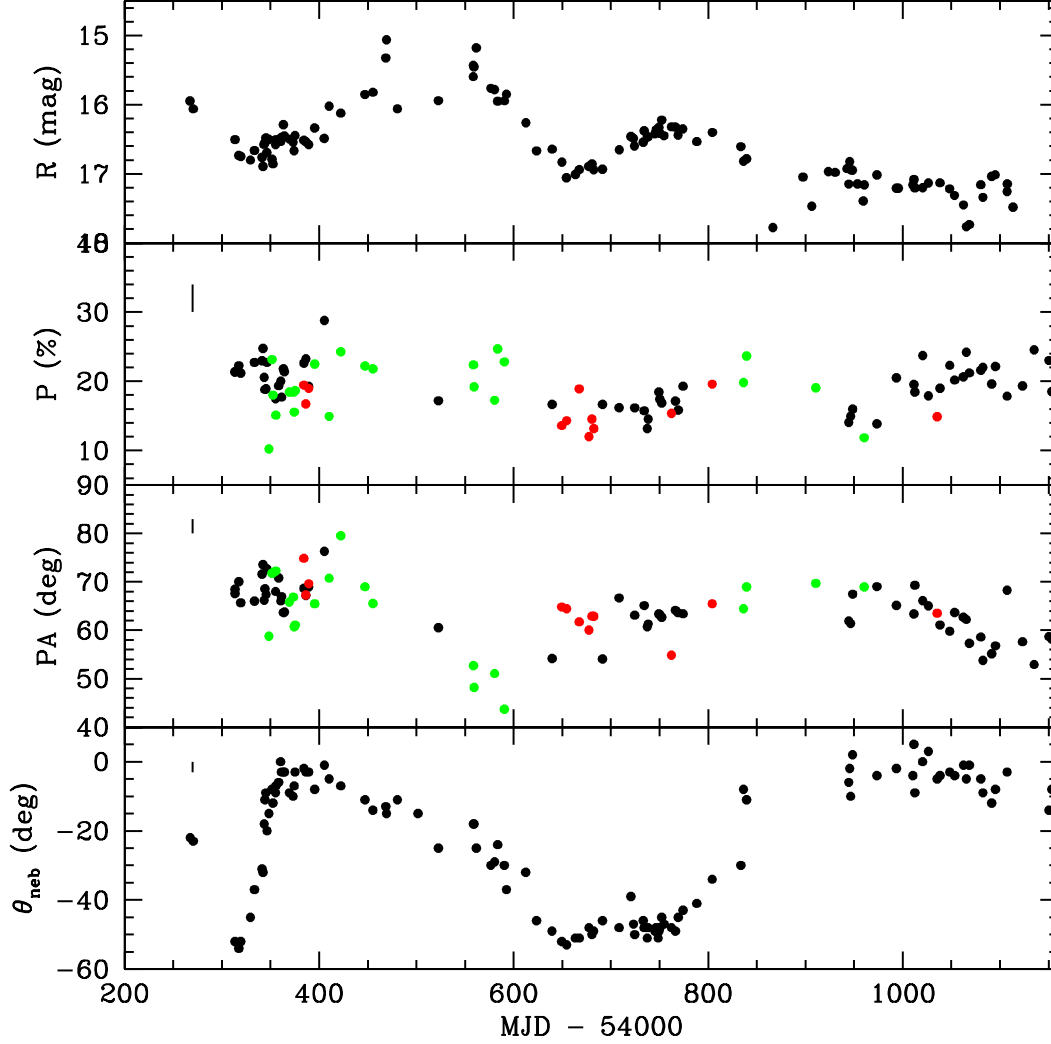


Fig. 5.— Temporal distribution of the PV Cep polarization intensity (in %, second panel) and position angle (PA in deg, third panel), along with the direction of the cometary nebula main axis (θ_{neb} , fourth panel). R (I) band polarization and PA values are depicted as red (black) dots, while green dots represent polarization and PA values obtained in unfiltered mode. The light-curve in the R band is plotted again (first panel), just for convenience. Typical errors are indicated by vertical bars in the upper left corner of each panel.

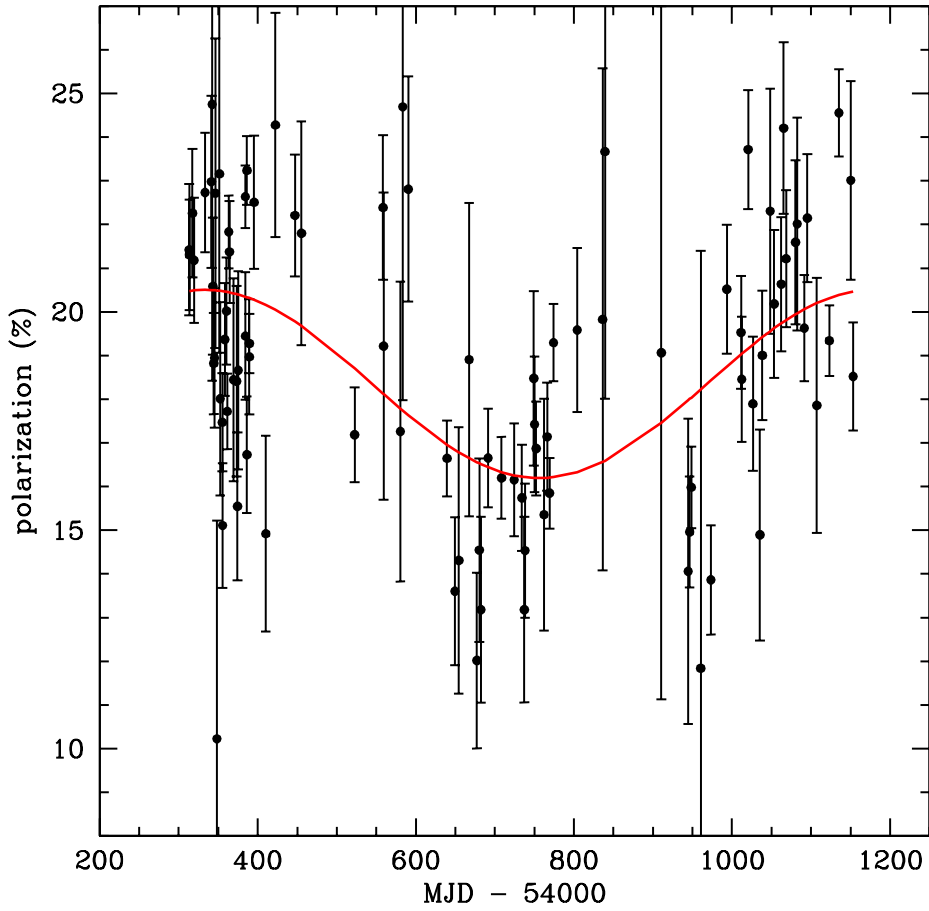


Fig. 6.— Temporal distribution of the PV Cep polarization intensity A sinusoidal fit to the data with period of 847 days and peak amplitude 2.1% is plotted, as well (red curve).

Table 1. Polarization measurements of PV Cep.

Date	λ (\AA)	P (%)	σ_P	PA (deg)	σ_{PA}	apert. (arcsec)	ref
1980 Oct 23	1.25 μm	11.9	1.1	101.4	—	—	1 (10.38 mag)
1980 Oct 23	1.65 μm	7.7	0.3	106.6	—	—	1 (8.48 mag)
1980 Oct 23	2.20 μm	3.9	0.1	107.2	—	—	1 (6.73 mag)
1981 Jun 21	1.25 μm	14.3	1.2	109.2	—	—	1 (10.76 mag)
1981 Jun 21	1.65 μm	9.1	0.2	111.4	—	—	1 (8.72 mag)
1981 Jun 21	2.20 μm	5.1	0.1	113.0	—	—	1 (6.77 mag)
1984 Jun	4000-10000	9.7	0.9	71	3	6	2
1986 Aug 5	7675	15.2	0.6	75.3	1.2	8.3	3
1986 Aug 10	7675	11.8	0.5	76.8	1.2	8.3	3
1986 Aug 12	7675	14.6	0.4	76.3	1.0	8.3	3
1986 Aug 13	4700	11.9	1.1	75.9	2.6	8.3	3
1986 Aug 12	7675	15.2	0.5	77.6	1.0	8.3	3
1989 Jul	4000-10000	16.2	0.3	89.9	0.5	6	2

^a References to the Table: (1) Lacasse 1982; (2) Scarrott et al. 1991; (3) Ménard & Bastien 1992.

Table 2. Observed Log of our observations of PV Cep.

Date	B	V	R	I	J	H	K	P_R	P_I	PA_R	PA_I	θ_{nebula}
(JD-2450000)	(mag)							(%)		(deg)		
4177						9.32						
4229					11.51	9.43						
4241					11.52	9.33	7.54					
4247					11.16	9.12	7.41					
4259					11.20	9.07	7.29					
4261					10.90	8.90	7.24					
4267	19.86	17.67	15.95	13.94	10.82	8.90	7.31					-22
4270	20.35	17.64	16.06	14.21								-23
4272					11.00	8.94	7.23					
4280					10.73	8.75	7.15					
4284					11.25	8.99	7.21					
4313	19.88	18.25	16.50						21.4		68.4	-52
4317		18.31	16.73						22.2		70.0	-54
4319		18.20	16.75						21.2		65.7	-52
4329		18.36	16.80	15.12								-45
4333		18.10	16.66	14.98					22.7		66.0	-37
4341		18.11	16.76						23.0		71.6	-31
4342		18.64	16.89	15.05					24.7		73.6	-32
4343		18.04	16.57	14.93					20.6		66.2	-18
4344		18.10	16.55	14.91					18.9		68.6	-11
4345		18.48	16.48	14.89					18.9		67.4	-9
4346		19.08	16.69	14.98					22.7		72.7	-20
4348		18.27	16.50	15.06				10.2*		58.8*		-15
4351			16.79	15.24				23.1*		71.7*		-8
4352			16.85	15.17				18.0*		71.9*		-12
4355	20.63	18.10	16.54	14.93				15.1*	17.5	72.2*	68.0	-8
4358			16.51	14.86					19.4		70.8	-6
4360		18.67	16.53	14.70					20.0		66.0	0
4361		18.04	16.48	14.71					17.7		67.0	-3
4363		17.95	16.29	14.33					21.8		63.6	-3
4364	19.52	18.02	16.45	14.46					21.4		63.8	-3
4369		18.41	16.50	14.68				18.4*		65.8*		-9
4373		18.08	16.54	14.66				18.4*		66.8*		-10
4374		18.24	16.66	14.55				15.5*		60.8*		-7
4375			16.45					18.6*		61.1*		-3
4382					11.59	9.25	7.30					
4384			16.51					19.4	22.6	74.9	68.6	-2
4385					11.39	9.12	7.24					
4386			16.53					16.7	23.2	67.2	67.2	-3
4388					11.41	9.05	7.12					
4389			16.58		11.53	9.13	7.27	19.0	19.3	69.6	68.9	-3
4390					11.47	9.05	7.21					
4395		17.92	16.37	14.42				22.5*		65.5*		-8
4398					11.07	8.86	7.09					
4401					11.14	8.88	7.11					

Table 2—Continued

Date	B	V	R	I	J	H	K	P_R	P_I	PA_R	PA_I	θ_{nebula}
4403					11.30	9.02	7.23					
4405			16.49						28.8		76.3	- 1
4409					11.50	9.00	7.10					
4410		18.13	16.02	14.54				14.9*		70.7*		- 5
4422		17.61	16.12	14.56				24.3*		79.5*		- 7
4447			15.85					22.2*		69.0*		-11
4455			15.82	13.92				21.8*		65.5*		-14
4468			15.32	13.77								-13
4469			15.06	13.53								-15
4480			16.06	13.83								-11
4501				13.38								-15
4522		17.52	15.94	14.23					17.2		60.5	-25
4557					10.27	8.29	6.70					
4558		17.24	15.43	13.35	10.09	8.12	6.54	22.4*		52.7*		-18
4559			15.45	13.36				19.2*		48.2*		-18
4561			15.18	13.24								-25
4564					9.98	8.16	6.46					
4569					10.14	8.13	6.57					
4576			15.76									-30
4580		17.32	15.78	13.74				17.3*		51.1*		-29
4583			15.95	13.93				24.7*		35.8*		-24
4590			15.94	14.12				22.8*		43.7*		-30
4592		17.39	15.85									-37
4595					10.85	8.54	6.76					
4612		17.59	16.26	14.56								-32
4613					11.36	8.93	7.08					
4614					11.45	9.01	7.08					
4623		17.94	16.67	14.97								-46
4627					11.96	9.36	7.38					
4630					12.27							
4631					12.36							
4633					12.34	9.71	7.62					
4634					12.35	9.73	7.68					
4636					12.34	9.74	7.73					
4637					12.40	9.79	7.72					
4639		18.23	16.64	15.00	12.19	9.63	7.58		16.6		54.1	-49
4641					12.23	9.62	7.54					
4642					12.28	9.62	7.53					
4643					12.17	9.55	7.51					
4644					12.04	9.48	7.43					
4645					12.08	9.54	7.55					
4646					12.00	9.48	7.47					
4648					12.03	9.54	7.55					
4649	18.81	18.36	16.83	15.11	12.02	9.54	7.56	13.6		64.8		-52
4650					12.06	9.54	7.50					
4651					12.12	9.59	7.54					

Table 2—Continued

Date	B	V	R	I	J	H	K	P_R	P_I	PA_R	PA_I	θ_{nebula}
4652					12.21	9.64	7.57					
4653					12.36	9.79	7.61					
4654		18.35	17.06	15.22	12.37	9.81	7.67	14.3		64.4		-53
4655					12.26	9.69	7.47					
4659					12.06	9.62	7.61					
4663		18.74	17.01	15.34								-51
4664					12.52	9.96	7.85					
4666	20.25											
4667		18.41	16.94	15.35				18.9		61.7		-51
4672					12.66	10.04	7.80					
4673					12.61	10.00	7.79					
4676					12.81	10.20	7.94					
4677		18.16	16.89	15.22				12.0		60.0		-48
4680		18.46	16.86	15.20				14.5		62.9		-50
4682		18.39	16.94	15.30				13.2		62.9		-49
4685					12.68	10.03	7.70					
4690					12.68	10.03	7.73					
4691		18.57	16.93	15.28					16.6		54.0	-46
4692					12.71	10.05	7.77					
4697					12.75	10.11	7.88					
4698					12.80	10.18	7.98					
4701					12.75	10.19	7.87					
4705					12.77	10.21	7.80					
4708		18.19	16.65		12.74	10.21	7.88		16.2		66.7	-48
4711					12.45	9.90	7.59					
4713					12.47	9.85	7.52					
4714					12.50	9.91	7.68					
4716					12.40	9.86	7.61					
4719					12.51	9.98	7.68					
4720		17.79	16.46	14.85	12.47	9.94	7.68					-39
4723		17.94	16.49	15.04								-47
4724			16.60	14.87	12.54	10.01	7.79		16.1		63.1	-50
4727			16.60	14.87	12.47	9.91	7.65					
4728			16.60	14.87	12.47	9.92	7.70					
4733			16.54	15.00								-46
4734		17.76	16.38	14.82					15.7		65.1	-48
4737		17.86	16.47						13.2		60.7	-51
4738		17.83	16.46	14.84	12.28	9.84	7.67		14.5		61.3	-48
4745		17.60	16.42	14.76								-49
4746		17.92	16.36	14.90								-48
4748		17.75	16.39	14.79								-51
4749		17.81	16.33	14.78					18.5		63.4	-49
4750		17.89	16.41						17.4		63.2	-48
4752		17.55	16.22	14.68					16.9		62.7	-45
4754			16.45	14.91	12.23	9.78	7.63					-47
4757					12.40	9.99	7.86					

Table 2—Continued

Date	B	V	R	I	J	H	K	P_R	P_I	PA_R	PA_I	θ_{nebula}
4759					12.22	9.78	7.64					
4760					12.21	9.77	7.68					
4762		17.66	16.32	14.76				15.3		54.8		-48
4765					12.09	9.67	7.43					
4766		17.92	16.32	14.76	12.13	9.71	7.68		17.1		64.1	-49
4769		17.87	16.44	14.83					15.8		63.6	-45
4772					12.25	9.87	7.78					
4773					12.12	9.71	7.66					
4774		17.90	16.35	14.75					19.3		63.4	-43
4779					12.04	9.66	7.61					
4780					12.20	9.81	7.80					
4781					12.16	9.83	7.81					
4782					12.13	9.83	7.85					
4788			16.53	14.86								-41
4790					11.86	9.73	7.80					
4804		17.81	16.40	14.77				19.6		65.5		-34
4833			16.61	15.05								-30
4836			16.82	15.12				19.8*		64.4*		- 8
4839			16.78	15.17				23.6*		68.9*		-11
4863				15.48								
4866			17.78	15.59								
4884					12.73	10.24	7.94					
4897			17.05	15.37								
4903					12.50	9.98	7.75					
4904					12.58	10.10	7.87					
4906			17.47									
4908					12.23	9.75	7.58					
4910				15.09				19.0*		69.7*		
4913					12.51	10.05	7.80					
4923			16.97	15.29								
4930			16.98	15.17								
4935				15.43								
4942			16.92	15.25								
4944			17.15	15.26					14.0		61.9	- 6
4945			16.82	15.10								- 2
4946		18.69	16.94	15.22					15.0		61.4	-10
4948		18.83	16.95	15.33					16.0		67.4	2
4953			17.14	15.24								
4959			17.39	15.34								
4960			17.16	15.36				11.8*		69.0*		
4973		18.56	17.02	15.27					13.9		69.0	- 4
4993		18.70	17.21	15.40					20.5		65.1	- 2
4995		19.18	17.21	15.55								
5010		18.89	17.16	15.49								- 4
5011		18.90	17.08	15.42					19.5		63.4	5
5012		18.83	17.20	15.44					18.4		63.3	- 9

Table 2—Continued

Date	B	V	R	I	J	H	K	P_R	P_I	PA_R	PA_I	θ_{nebula}
5020		18.73	17.20	15.40					23.7		66.1	0
5026		18.71	17.13	15.42					17.9		65.0	3
5035	19.99	18.77		15.39				14.9		63.5		- 5
5038			17.13	15.45					19.0		61.1	- 4
5048			17.22	15.67					22.3		59.8	- 3
5053			17.31	15.54					20.2		63.7	- 4
5062			17.45	15.77					20.6		62.7	- 1
5065			17.76	15.95					24.2		62.2	- 5
5068			17.73	15.94					21.2		57.3	- 1
5080			17.16	15.19					21.6		58.6	- 5
5082			17.34	15.28					22.0		53.8	- 9
5091			17.04	15.01					19.6		55.2	-12
5095			17.01	15.12					22.1		56.8	- 8
5107		19.27	17.25	15.39					17.9		68.2	- 3
5113			17.48	15.41								
5123			17.48	15.41					19.3		57.6	
5135			17.48	15.41					24.5		52.9	
5150			17.48	15.41					23.0		58.7	-14
5153			17.48	15.41					18.5		58.2	- 8

^aTypical errors of the optical (near/IR) magnitude never exceed 0.02 mag, while errors on P and PA are of the order of 1-3 % and 2-4°, respectively. The uncertainty of θ_{nebula} is about 1-2°.

^bPolarization and PA values obtained in unfiltered mode.